Research article

A comparison study between CFD analysis and PIV technique for velocity distribution over the Standard Ogee crested spillways

Rizgar Ahmed Karim [a,*], Jowhar Rasheed Mohammed [b]

[a] University of Sulaimani, Sulaimani, Iraq
[b] University of Duhok, Duhok, Iraq

A B S T R A C T

A comprehensive study was performed to compare flow rate, mean velocity, vertical velocity distribution, and locations where the maximum velocity, d_m, occurs on standard Ogee-crested spillways using experimental and numerical models. Five different models were constructed from rigid foam according to the specifications of the United States Army Corps of Engineers (USACE). The velocity of the flow was recorded along the downstream curve of the model for all models with different non-dimensional head ratios H/H_d of 0.50, 1.00, and 1.33. Particle Image Velocimetry (PIV) was used to measure the flow velocities. Velocity distributions were obtained by analyzing a series of captured images using Matlab codes. A commercially available Computational Fluid Dynamics (CFD) software package, Flow-3D, was used for modelling the experimental model setups. Flow-3D analyzes the Reynolds-averaged Navier-Stokes equations and is widely verified for use in the field of spillway flow analysis. The maximum difference between numerical and experimental results in mean velocity values that do not exceed 6.2% for all values of head ratios. The interpolated values of recorded maximum velocity by the PIV technique are smaller than those values numerically computed. In the lower d_m locations, the percent difference between these regions reaches -8.65%; the upper locations are 2.87%. The vertical location (d_m) drops to the lower location when the upstream head increases, and the distance from the spillway axis decreases linearly.

1. Introduction

The Ogee-crested spillway is one of the most important and common hydraulic structures, its superb hydraulic characteristics allow it to release excess water or floods that cannot be contained in the storage volume. Ogee-crested spillways are common as water discharge structures in various situations (U.S. Bureau of Reclamation, 1987). They are efficient and safe when designed and built with precision; they also measure the flow rates with sufficient precision. When the pressure head reaches a design head, a zero relative pressure is often found along the surface profile (Peltier et al., 2018). However, an improper design of this structure can lead to dam-break. National statistics shows that overtopping due to inadequate spillway design, debris blockage of spillway, or settlement of the dam crest account for approximately 34% of all dam failures in the United States of America; thus, these spillways have to be carefully designed to verify flow characteristics (Engineers, 1952). Experimental models facilitate experimental studies of flow over a spillway, and the results can give reliable information for proper spillway design (Willey et al., 2012).

The ogee-crested spillway is one of the most studied hydraulic structures because of its performance and its ability to pass surplus water efficiently and safely with reasonably good flow measurement capabilities. Thus, engineers use it in a wide range of situations (Savage and Johnson, 2001). Flow over the Ogee-crested spillway should adhere to the face of the profile to prevent entrance of air underneath the water sheet. In terms of head design, the flow glides over the surface profile with minimal boundary surface interference; this leads to an optimum efficiency of discharge (Kanyabujinja, 2015).

There are relatively few studies on the flow characteristics over an Ogee crested spillway, particularly for heads that are larger than the design head. There is also no sufficient information available regarding the vertical velocity distribution along the crest profile. Peltier et al. (2015) validated pressure measurements and velocity distributions conducted in two hydraulic models with various scale factors of an Ogee spillway. These were operated at head ratios that are largely greater than unity (Peltier et al., 2018).

Numerical simulations are useful in hydrodynamic studies including studies of flow over Ogee spillways. A comparison of these numerical

---

* Corresponding author.
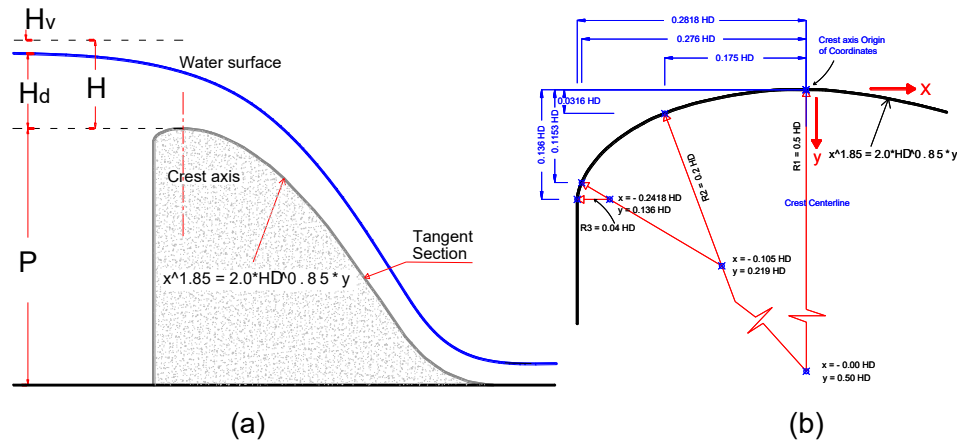*E-mail address:* rizgar.karim@univsul.edu.iq (R.A. Karim).

Figure 1. Dimensions of standard ogee-crested spillway, (a) dimensions and flow parameters, and (b) detail of upstream quadrant.

results with experimental data is still required for calibration and validation. The commercially available Computational Fluid Dynamics software package, Flow-3D, uses the finite-volume method and can solve problems involving fluid flow. The computational domain is subdivided using Cartesian coordinates into a grid of variable sized hexahedral cells. For each cell, the average values for the flow parameters such as pressure and velocity are computed at discrete times. Most literature on CFD-based modeling of spillways uses Flow-3D, which solves the Reynolds-averaged Navier-Stokes (RANS) equations (Chanel and Thesis, 2009; Ho et al., 2006; Kim and Park, 2005; Savage and Johnson, 2001).

PIV is a type of pulsed light velocimetry (Adrian, 1991; Sveen and Cowen, 2004). It uses a particulate tracer to track fluid displacement. The PIV technique is based on the measurement of small tracer particles. These are sufficiently small to follow the movement of the fluid of interest. These particles are then illuminated with a thin light sheet. Scattered light was then stored in subsequent image frames with known intervals using a camera. PIV measures the entire velocity field and calculates the displacement of the particles within the given time frame by taking two images instantaneously after each another with high-speed camera (Fujita et al., 1998). These recorded images are then processed on a computer using Matlab codes to analyze the movement of particles in subsections of the PIV images via cross correlation techniques. The result leads to a particle-image displacement pattern after considering the image magnification and time delay (Kuok and Chiu, 2017).

Several studies have worked to improve the performance of the Ogee-crested spillway to release surplus water. Peltier et al. (2015) measured the velocity field via a large-scale particle image velocimetry (LSPIV): The results showed that the relative flow velocity is indeed slightly higher for the greater spillway size.

This study describes a hybrid model approach to measure flow over an Ogee-crested spillway. The approach involves velocity measurements using the PIV technique-a well-established technique in laboratory-based fluids research. CFD models were also used to compare the experimental model tests with CFD results. The findings help explain how accurately a

CFD model can predict the mean velocity and vertical distribution of velocity along the downstream curve of the spillway.

2. Material and methods

2.1. Experimental model

Various shapes and designs of the ogee spillways have been proposed. Most variations are on the curves upstream of the crest axis. Crest shapes have been studied extensively at USBR laboratories using experimental data with a variety of upstream water depths. The upper nappe was carefully measured for various discharges and velocities (Khatsuria, 2004).

Maynord (1985) showed four different shapes of the upstream face of the spillways: one vertical and three inclined. The upstream curve profile is a combination of radii that are relative to the total head, while the downstream curve is the portion between the crest axis and the tangent section. The vertical upstream face type was standardized via the equation below:

$$X^{1.85} = 2.0 H_d^{0.85} * Y \tag{1}$$

here, H_d is the design head above the crest, and X and Y are coordinates of the crest profile with their origin at the highest point of the spillway crest (Engineers, 1952). The Cartesian coordinate system (x, y, and z) described the stream-wise, vertical direction, and span-wise, respectively; (x, y, z) = (0, 0, 0) at the crest. The y-axis is directed in the downward direction.

One of the main objectives of this study is to reproduce flow over the Ogee crested spillway in a controlled environment for heads higher than the design head while also selecting the vertical location for maximum velocity.

To achieve this, five experimental models with a vertical upstream face and a height sufficient to ensure negligible approach velocity were constructed (Figure 1).

Table 1. WES standard upstream spillway quadrant for vertical upstream face.

| Model No.	Design Head, H_d (cm)	Spillway Height, P (cm)	Spillway crest Length, L (cm)	Coefficient of Discharge, C_d	Length of Quadrant Radii (cm)			The Endpoint of the Downstream Curve (cm)		Design Discharge (l/sec)
					R_1	R_2	R_3	x	y	
1	9.0	20	29.24	0.492	4.50	1.80	0.36	12.82	11.34	18.6
2	7.5	20	27.83	0.493	3.75	1.50	0.30	10.68	12.78	13.5
3	6.0	20	26.42	0.493	3.00	1.20	0.24	8.56	14.21	9.75
4	4.5	20	25.03	0.493	2.25	0.90	0.18	6.41	15.67	6.30
5	3.0	20	23.62	0.493	1.50	0.60	0.12	4.27	17.11	3.40
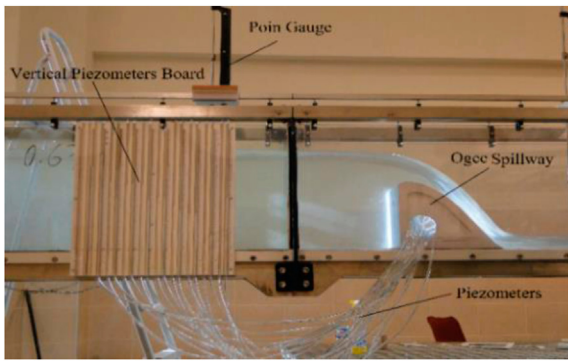
Figure 2. Side view of the experimental model.
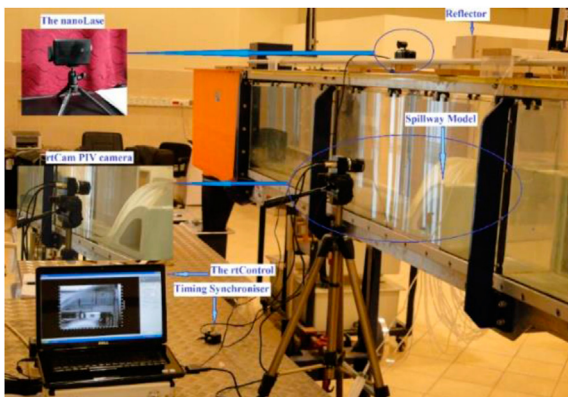
Figure 3. Laboratory setup.

The upstream curve consists of three different radii curves. The smaller radius curve ($R_3 = 0.04*H_d$) is connected with the curved portion of the crest to the upstream vertical face; this vertical face was added to eliminate the surface discontinuity and improved the pressure conditions and discharge coefficients at heads exceeding the design head.

All models were designed and constructed as shown in Table 1. The equation used for the design of the downstream crest profile is from Maynord:

$$y = \frac{x^{1.85}}{2H_d^{0.85}} \tag{2}$$

The experimental models are made of rigid foam and constructed using the computer numerical control (CNC) machine to conform to the

distinctive shape of an ogee spillway. The CNC machine represents an actual programmable machine capable of performing numerical control machining operations autonomously. Rigid foam is selected because it can be fabricated with smooth curves. Each model is installed in the flume at the middle of a glass panel to visualize the process of testing and profile measurements, as shown in Figure 2.

The experimental flume (S6-MKII) is a glass-sided tilting flume with a bed of stainless steel. It has a working cross-section of 300 mm by 450 mm deep and is available in a standard working length of 7.5 m [Instruction manual of S6-MKII, Armfield Company (2014)].

2.2. Measuring techniques

Each of these models was placed in a testing flume 4.0 m from the upstream end. The flow dynamics were measured in each model and analyzed for three head-ratios H/H_d (0.50, 1.00, and 1.33). The discharge passing over the models was measured using the electromagnetic flow-meter provided. The depth of water in the flume that passed over the models is measured with two-point gauges. The precision of the measurement was estimated to be ± 0.1mm via calibration testing. The velocity of different points on the surface of the spillway models is measured using PIV techniques.

PIV is a flow field technique that offers instantaneous velocity vector measurements in a cross-section of the flow. Here, only two velocity components are measured. The use of a stereoscopic approach permits all three velocity components to be recorded resulting in instantaneous 3D velocity vectors for the entire study area. This technique was selected to obtain a non-intrusive time series allowing analysis of spatial-temporal characteristics of the flow (Adrian et al., 2011).

The rtCam PIV system version 1.3 was used for velocity field measurements on the spillway crest. A double pulse laser operating at a maximum of 15 Hz and manufactured by Etalon Research was also used as shown in Figure 3.

The laser had a pulse width of 3–5 ns and a beam diameter of 4.0 mm producing a red light of 600 nm. This system was used to record two velocity components (u, stream-wise and v, vertical direction) within the plane of symmetry on the crest [Manual of the rtCam PIV System (2009)].

The rating curve of the spillway is an important hydraulic characteristic that shows the consistency and accuracy of the model. It is calculated from theoretical equations. The data is recorded with an electromagnetic flowmeter and then compared with the equation. The flowmeter was settled under the flume to be connected between the centrifugal pump and the molded inlet tank. The theoretical discharge through the ogee-crested spillway can be expressed as described (Savage and Johnson, 2001):
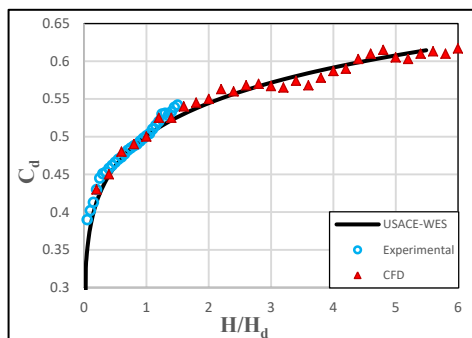
(a) Model No. 1
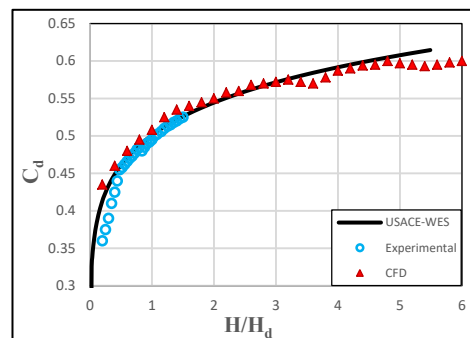
(b) Model No. 3

Figure 4. Discharge Coefficients of Experimental and Numerical results plotted together with USACE-WES Published Data, (a) for model No. 1, (b) for model No. 3.
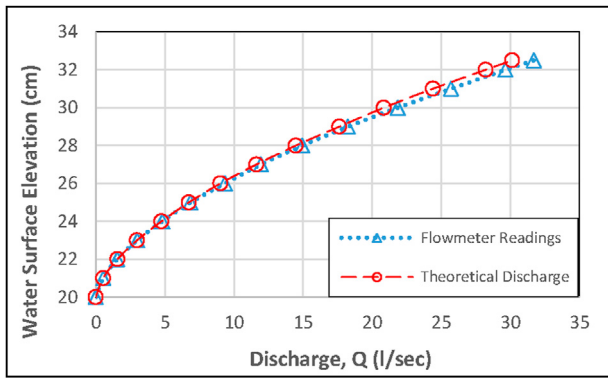
Figure 5. Rating curves of theoretical discharge and flowmeter reading.
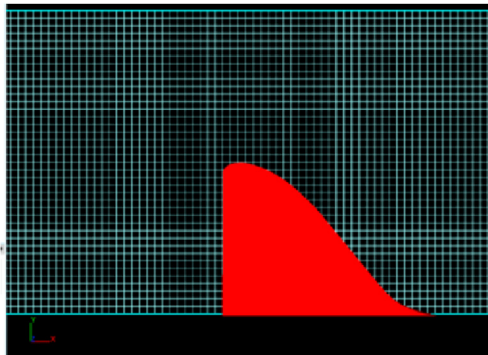

Figure 6. Mesh geometry.

$$Q = \frac{2}{3} CL\sqrt{2g}H_e^{3/2} \tag{3}$$

here, Q denotes the total discharge, and C is a coefficient of discharge; $g =$ gravitational acceleration, L is the lateral crest length of the spillway, and H_e is the total head measured upstream from the crest to the unaffected upstream water stage including the velocity head. The Variation range of C is between 0.578 and 0.75 or so and corresponds to the highest acceptable value without exceeding the allowable sub-atmospheric pressure on the crest.

$$Q = C_d L H_e^{3/2} \tag{4}$$

where $C_d = \frac{2}{3} C \sqrt{2g}$

The coefficient of discharge C_d is not a dimensionless quantity. Its standard value for the design head is 3.98 in British units, which is equivalent to 2.198 in metric units (Khatsuria, 2004).

Figure 4 compare discharge coefficients with respect to head ratio (H/H_d) using the vertical upstream face. The published data of USACE-WES was used as a baseline for comparison. This comparison indicates good agreement because the absolute difference between WES with the

experimental and numerical results does not exceed 2.76%; the absolute difference between experimental and numerical results was 1.66%.

The discharge coefficient is not constant, it is influenced by several factors including the depth of the approach (as shown in Figure 4), relation of the actual crest shape to the ideal nappe shape, upstream face slope, downstream apron interference, and downstream submergence.

Figure 5 compares the theoretical discharge and flowmeter reading for Model No. 1. Both values are very close to each other, and the maximum difference between them does not exceed 5.11% when the discharge is higher than 10 l/s. For a particular discharge, the flow can pass over the spillway with lower flow depths than the theoretical discharge.

3. Numerical model

The CFD model included the symmetric representation of the ogee spillway in three dimensions. Flow-3D uses VOF to interface and capture the scheme for the free surface flow where the interface of each fluid is the point of focus. The model solved the field of turbulent flow based on continuity equation and Reynolds-Averaged Navier-Stokes (RANS) equations to minimize the effects of rapid fluctuations.

The mesh process is a very important stage that requires a lot of attention in CFD modeling. The domain had to be divided into smaller cells to analyze the fluid flow in which the governing equations would be solved as shown in Figure 6. The number and size of the cells are important criteria for the simulation of numerical model and restrict the accuracy of the results and the time of simulation.

A suitable method to determine the critical mesh size is to begin with a relatively large mesh and then reduce it until the desired efficiency is reached; further size reductions have no effect on the results.

The determination of the correct mesh domain along with an acceptable mesh size is a critical part of any numerical model simulation. Mesh and cell size can affect both accuracy and simulation time; thus, it is important to minimize the number of cells while having sufficient resolution to capture the important features of the geometry as well as sufficient flow detail.

Here, the size of the cells has been continuously reduced, and the time elapsed for simulations has been considered such that the reduction in size does not affect the accuracy of the results.

The mesh sizes used in this study were 1 cm and 0.5 cm in all directions and for all models. These were then reduced to 0.33 cm to provide more accurate results for the flow characteristic tests. The three-dimensional domain was -200 < x < 100, 0 < y < 40, 0 < z < 30 cm.

The total number of elements used in the tests as well as the active and passive elements with the elapsed times for all models are shown in Table 2.

The general equations governing RANS and continuity equations for incompressible flow including the FAVOR variables are given by:

$$\frac{\partial}{\partial x_i}(u_i A_i) = 0 \tag{5}$$

Table 2. The Total Number of Elements, Number of Active Elements and Elapsed Times for Mesh Size of 0.33 cm.

| Model No.	Element Numbers in Direction			Total Number of Elements	Number of Active Elements	Number of Passive Elements	Elapsed Time day:hr:min:sec
	x	y	z				
1	900	87	90	7047000	4102233	2944767	01:06:03:35
2	900	83	90	6723000	3913624	2809376	01:02:41:36
3	900	78	90	6318000	3677865	2640135	00:19:50:47
4	900	74	90	5994000	3489255	2504745	00:15:25:48
5	900	69	90	5589000	3253495	2335505	00:16:39:31
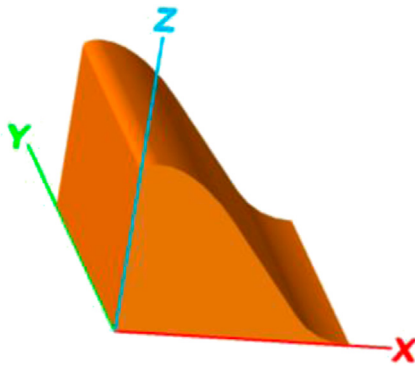
Figure 7. Numerical model geometry.
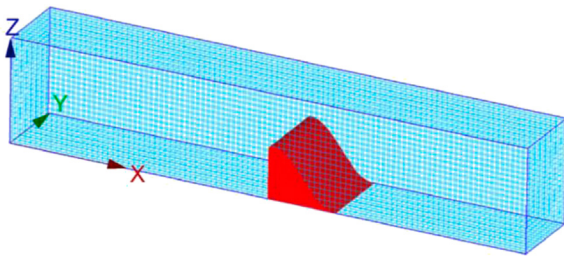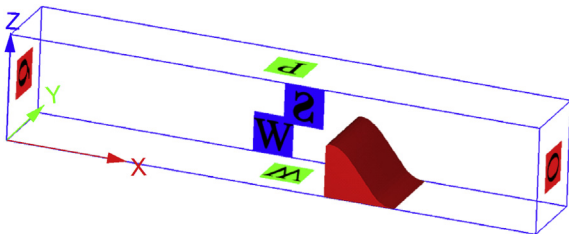

Figure 8. Mesh geometry.

Figure 9. Boundary conditions of the Modeling.

$$\frac{\partial u_i}{\partial t} + \frac{1}{V_F}\left(u_j A_j \frac{\partial u_i}{\partial x_i}\right) = \frac{1}{\rho}\frac{\partial p}{\partial x_i} + g_i + f_i \tag{6}$$

here, u_i represents the velocity in the x_i ($i = 1, 2, 3$) directions (x, y, z directions); t is time; A_i is fractional areas open to flow in the subscript directions; V_F is a volume fraction of fluid in each cell; ρ is density; p is hydrostatic pressure; g_i is gravitational force in the subscript direction; and f_i is the Reynolds stresses for which a turbulence model is required for closure.

The main setup was the same for all models. Each run applied one fluid, incompressible flow, and a free surface. The water was set to 20 °C for all simulations. The gravity option was activated with gravitational acceleration in the y-direction set to (-981 cm/s^2). The viscosity and turbulence options were also activated with Newtonian viscosity being applied to the flow along with a selection of appropriate turbulence. The turbulence option used the two equations (k-ε) model. Non-slip or partial slip was used for wall shear boundary conditions.

A numerical model geometry was prepared by drawing spillway models using AutoCAD in a 3D form (Figure 7). These were exported into the stereo lithography (STL) format and then directly imported into Flow-3D where the appropriate mesh was generated.

Here, the origin of the domain is positioned at the bottom of the flume at one side of the vertical face of the spillway model. The x component represents the longitudinal direction along the flume, the y component
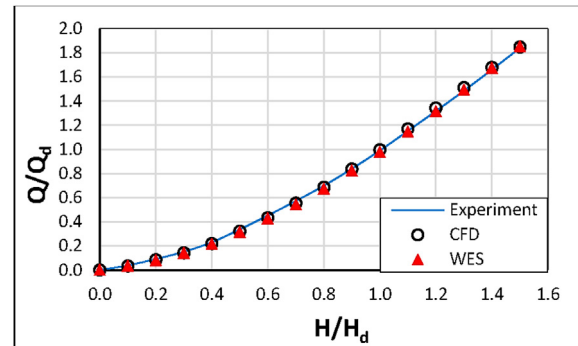

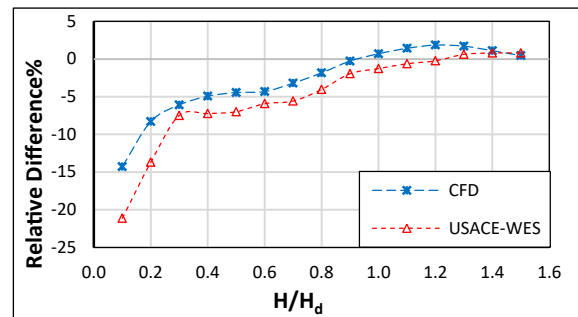**Figure 10.** Normalized discharge comparison.

Figure 11. Relative percent difference in discharge.

represents the change in vertical distance, and the z component represents the lateral direction with respect to the origin as shown in Figure 8.

The boundary conditions are the same for all models and were established as follows: The x minimum boundary is set as a volume flow rate (Q), the x maximum boundary was set as outflow (O). The y minimum boundary was set as the wall (W), and the y maximum boundary is set as the specified pressure (P). The z minimum boundary is set as the wall (W), and the z maximum boundaries are set as symmetry (S) as shown in Figure 9.

4. Results

The main purpose of this study is to compare the experimental results with the numerical results for flowrates over the models, depth-averaged velocity distributions, and vertical distributions of velocity.

4.1. Flow rate

The flowmeter reading (Q_{flow}) was compared to the numerically computed discharge (Q_{cfd}). The results were normalized to compare systems in the simplest form (Figure 10); published data of USACE-WES was used for the sake of additional comparison.

Figure 10 shows that the total head (H) above the crest is normalized via the design head (H_d) and shown in the abscissa. The discharge (Q) is normalized by design discharge (Q_d) and is shown on the ordinate. The experimental results were used as a baseline for comparison. This comparison shows good agreement and the maximum difference between experimental and numerical results does not exceed 5.59%. The maximum difference between the normalized WES published data and the experimental results was -7.54%.

The values of actual non-dimensional discharges are included in the inset. The experimental model and its discharge are used as the observed standard in this study. The relative percent difference is shown in Figure 11. The relative percent difference in discharge, at a given (H/H_d), is defined as below:
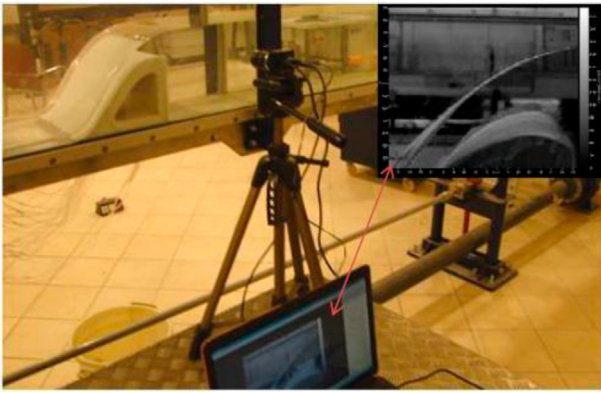
Figure 12. Experimental set-up of particle image velocimetry (PIV) system.

$$Relative\ \ Difference\ \% = \left(\frac{Q_{cfd} - Q_{flow}}{Q_{flow}}\right)*100 \qquad (7)$$

here, Q_{flow} is the flowmeter reading, and Q_{cfd} is the numerically computed discharge or as interpolated from the USACE-WES.

The relative percent difference depicted in Figure 11, shows that the numerical result agrees on average to within 2.45% of the experimental results. The numerical model flowrate is similar to that published by the USACE-WES, but has a slight reduction in the accuracy.

4.2. Mean velocity

For all the experiments, the mean velocities were recorded via a PIV camera. This camera is used to capture images of seeded water that flow over the model during the test. The solution of water and seeding particles was prepared previously. The diameter of seeding particles used here was 100 μm and the density of the concentrated solution was 1.015 g/cm^3.

Figure 12 illustrates the experimental setup of the PIV camera and its accessories; this also shows the spillway model fixed inside the exposed and uncovered testing flume.

Figure 13 illustrates the seeded water flow over a spillway model on the left-hand side and the raw image and post-processed images on the right-hand side.

Matlab software uses cross-correlation in image processing. The peak matching point of the cross-correlation gives the displacement distance while the known time between pairs of images allows for derivation of a velocity vector as shown in Figure 14. A velocity field is generated for every pair of frames.

Particle Image Velocimetry enabled us to measure the field of velocity and the streamlines over the flow over the surface of the ogee spillway. The laser light sheet direction is vertical and stream-wise at the surface centerline. Figure 15 demonstrate the velocity vector field together with the streamlines and present the free surface flow profile for approximation flow of q = 18.6 and 9.75 l/sec per meter length. Data consists in a steady-state test with an approximate duration of each test was about 15 s. In the laboratory the free water surface is measured with good
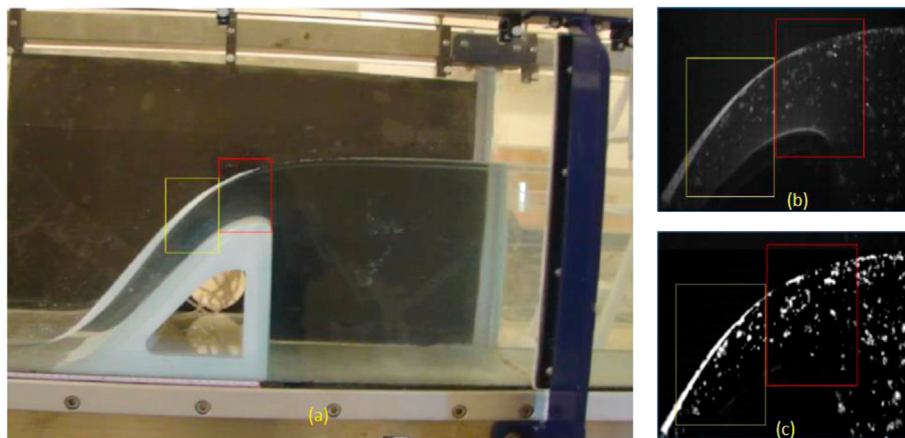

Figure 13. (a) Spillway Model setup, (b) Raw Image, and (c) Post-processed Image.
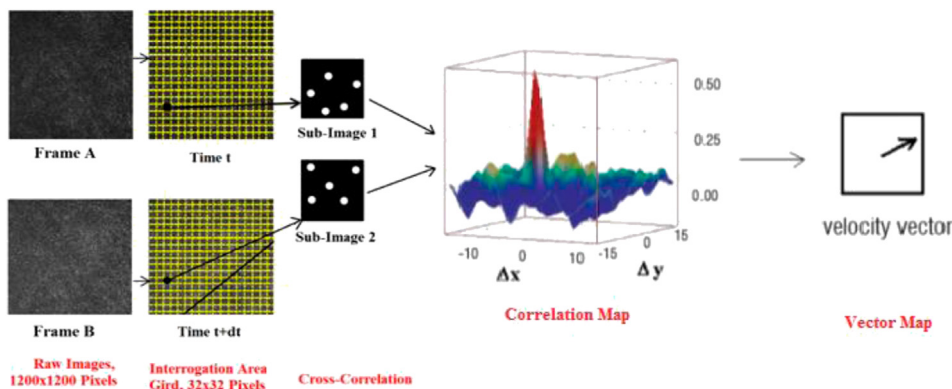

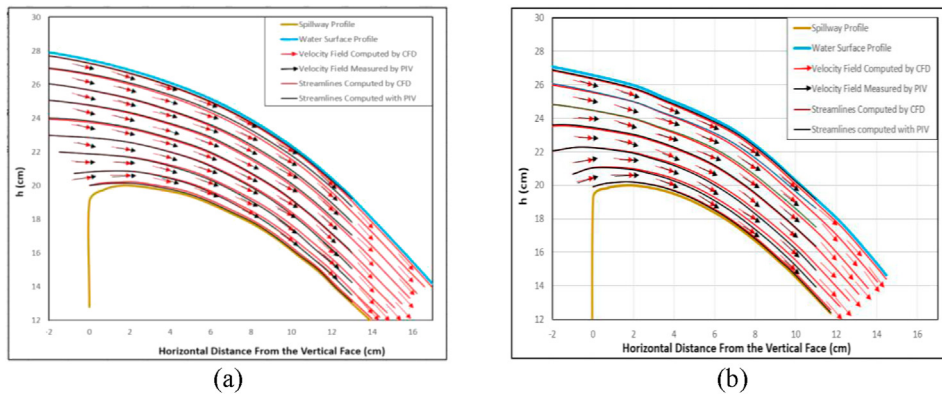**Figure 14.** Cross-correlation algorithm.

Figure 15. Velocity field and streamlines measured by PIV and simulated with CFD for flow over ogee spillway, (a) model no. 1 and (b) model no. 3.

(a) Model No. 1, H/H$_d$ = 0.50

(b) Model No. 1, H/H$_d$ = 1.00

(c) Model No. 1, H/H$_d$ = 1.33

(d) Model No. 2, H/H$_d$ = 0.50

(e) Model No. 2, H/H$_d$ = 1.00

(f) Model No. 2, H/H$_d$ = 1.33

(g) Model No. 3, H/H$_d$ = 0.50

(h) Model No. 3, H/H$_d$ = 1.00

(i) Model No. 3, H/H$_d$ = 1.33

(j) Model No. 4, H/H$_d$ = 0.50

(k) Model No. 4, H/H$_d$ = 1.00

(l) Model No. 4, H/H$_d$ = 1.33

(m) Model No. 5, H/H$_d$ = 0.50

(n) Model No. 5, H/H$_d$ = 1.00

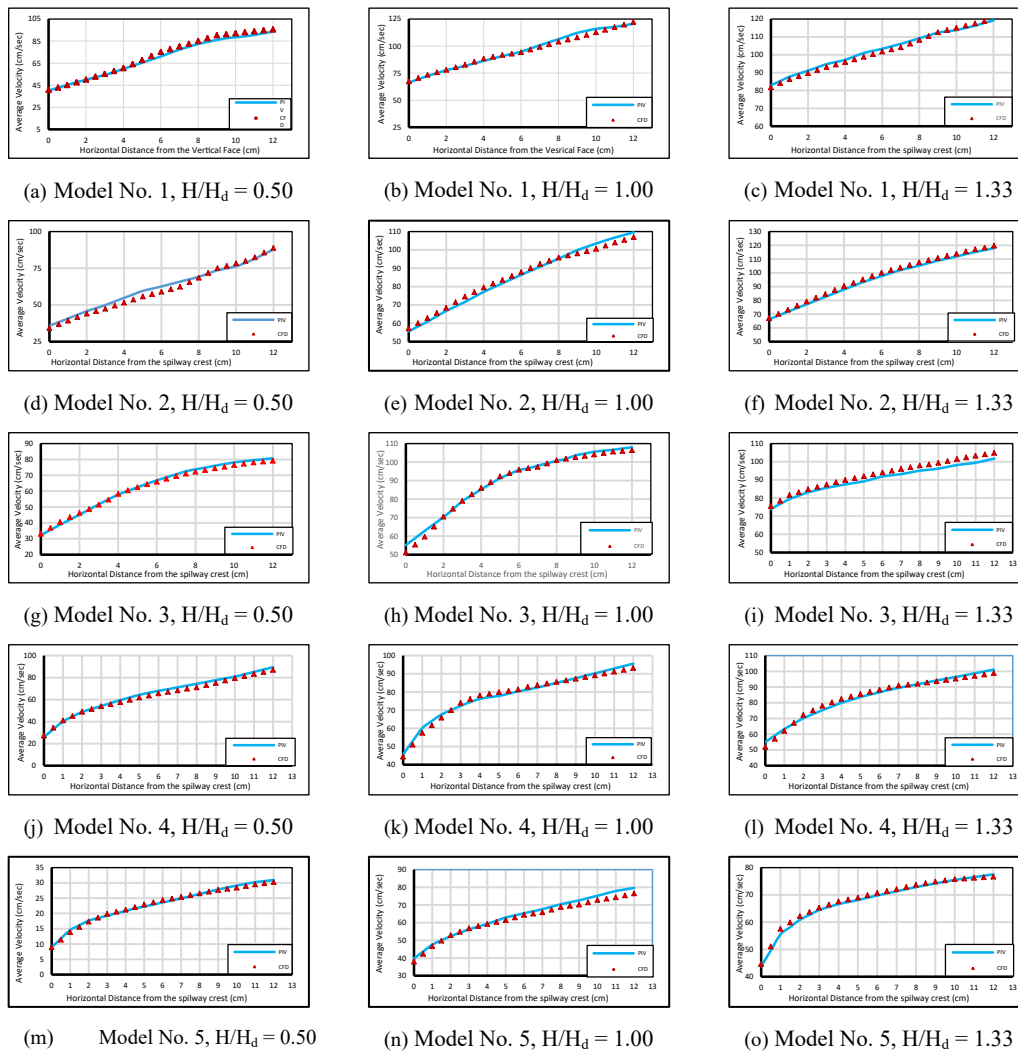(o) Model No. 5, H/H$_d$ = 1.33

Figure 16. Comparison of head-mean velocity of experimental and numerical analysis for all models.

agreement to the numerical simulation of the CFD. Velocities and streamlines show good agreement between the observed and estimated values.

For each model, the mean velocities were recorded using the PIV camera and analyzed numerically in the CFD model for three head-ratios H/H$_d$ (0.50, 1.00, and 1.33) as shown in Figure 16. The comparison results between numerical results and experimental data recorded by PIV camera show good agreements for all head-ratios. The maximum differences were 6.54% for a head-ratio of 0.50; 6.08% at a head-ratio of 1.00; and 5.52% at a head-ratio of 1.33. The results suggest good agreement between experimental and numerical results. The mean velocity increases with increasing H/H$_d$ and flowrate.
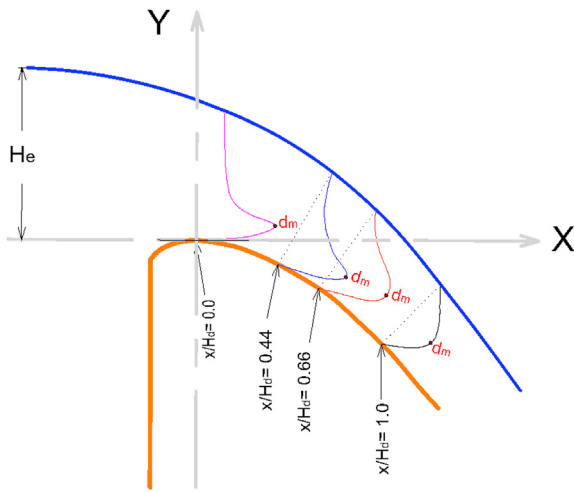
Figure 17. Sketch of velocity profile and its position for model no. 1.

4.3. Vertical distribution of velocity

A PIV camera was used to measure the flow velocity. The vertical distribution of velocity was obtained by analyzing a series of images with Matlab. The velocities are recorded via PIV techniques for five models with different design heads.

Figure 17 shows a vertical distribution of velocity and its locations for velocities recorded by PIV camera, also shows the position of the maximum velocities, d_m. This figure represents the data of Model No. 1 under a head ratio ($H/H_d = 1.33$) at locations ($x/H_d = 0.0$, 0.44, 0.66, and 1.00) from the apex of the spillway model.

Figure 18 presents the vertical distribution of velocity over the standard USACE-WES ogee-crested spillways for different head-ratios
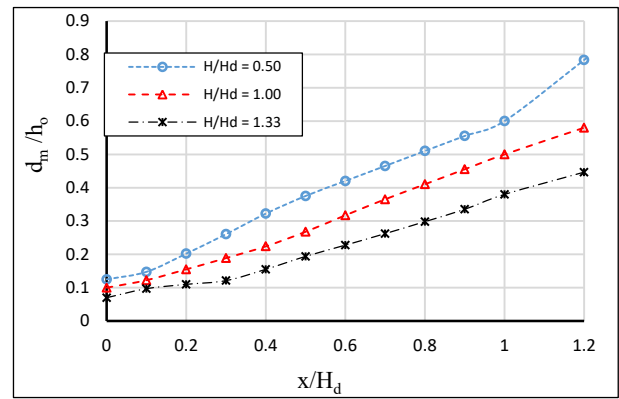

Figure 19. Vertical location of maximum velocity.

(1.33, 1.00, and 0.50); these plots are dimensionless. Here, v_{max} is the maximum velocity that occurs at location d_m for any section (x/H_d). Term h is the depth of flow, and h_o is the water depth measured perpendicularly from the spillway surface.

The interpolated value of velocity ratio ($v/v_{max.}$) of the flow recorded with PIV is smaller than that calculated numerically with the CFD model in the lower locations of d_m. The percent difference of the velocity ratio below the d_m location was -8.65%. In the upper locations of the d_m, the interpolated velocity ratio of the flow with the PIV technique is larger than that with numerical results. The percent difference of the velocity ratio above the location of d_m between experimental and numerical was 2.87%. This phenomenon occurs because the surface roughness was not considered in numerical modeling. At the beginning, the flow is accelerated at the bottom layer of the spillway surface. Over time, the flow at the free surface is increasingly accelerated past the crest axis. After
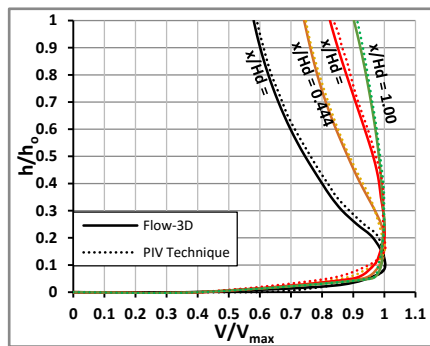
(a) Model No. 1, $H/H_d = 1.33$
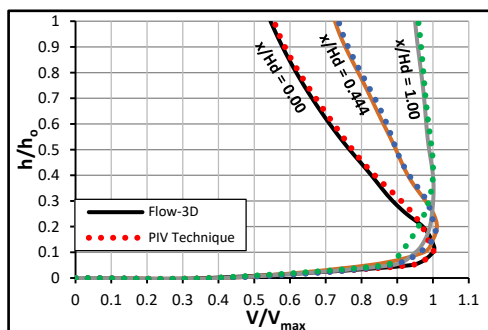
(b) Model No. 1, $H/H_d = 1.00$
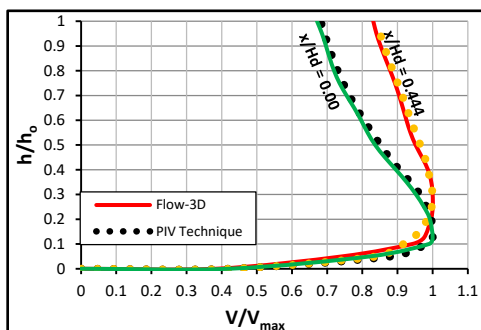
(c) Model No. 1, H/Hd = 0.50

Figure 18. Vertical Distribution of Velocity for Different Runs of model No. 1.

passing the crest axis, the flow quickly evolved to a logarithmic distribution as shown in Figure 17.

Figure 18 also compares the vertical distribution of velocities recorded by a PIV camera and those calculated with the CFD program. This figure presents the data of model No. 3 under a head-ratios ($H/Hd = 1.33$) at locations ($x/H_d = 0.0$, 0.44, 0.66, and 1.00) from the apex of the spillway model.

The vertical distribution of velocity for these three head ratios are depicted in Figure 18. The results show that the general tendency of the velocity distribution is almost the same. A comparison between the recorded data by the PIV camera and numerically computed data with Flow-3D shows good agreement between experimental and numerical results; thus, the Flow-3D can nicely simulate the vertical distribution of velocity.

4.4. Maximum velocity location

The vertical locations with the highest velocity are illustrated in Figure 19 for H/H_d of 0.50, 1.00, and 1.33 in a dimensionless form. The vertical positions are relative to the location of the upstream water head, H_o. The figure also shows the vertical location where the maximum velocity occurs, this location is at a lower position as the upstream water head increases. This location increases almost linearly with distance from the spillway axis.

5. Conclusions

This study has been conducted as a contribution toward a better understanding of flow over the Ogee crested spillway in a controlled environment for heads higher than the design head while also selecting the vertical location for maximum velocity. Here, five experimental models were designed and constructed according to the USACE-WES standard spillway shapes and tested in a laboratory flume. The PIV camera was used to measure the flow velocities and CFD software was used for modelling the experimental setups.

The numerical results agreed well with experiments. The rating curve results show that the maximum difference between numerical and PIV values suggests that mean velocity values do not exceed 5.59% for all values of head ratios. The maximum difference between normalized WES published data and the experimental results was -7.54%.

Recorded mean velocities with the PIV camera were analyzed numerically in the CFD model, and the comparison results show that there is good agreement between numerical and experimental data; the maximum difference does not exceed 6.54% for all head ratios.

The experimental interpolated data of the velocity ratio ($v/v_{max.}$) are smaller than those computed numerically in locations below d_m, but this is conversely in locations higher than the dm. This phenomenon occurs because the surface roughness was not considered in numerical modeling. The surface of the spillway models was assumed as smooth surface. The vertical position on which maximum velocity occurs is located at lower position as the upstream water head increases. The location almost linearly increases with distance from the spillway axis.

The required mesh refinement and configuration varies depending on the type of data desired. In general, a 0.33 cm mesh was sufficient for modeling velocity profile, we also evaluated a smaller grid size, but there was no change.

With respect to the comparison between experimental and numerical modeling, it is clear that experimental modelling is still more established. Although CFD models can provide more detail about velocity and turbulence than an experimental model, it may be more economical in some cases.

Declarations

Author contribution statement

Rizgar Ahmed Karim & Jowhar Rasheed Mohammed: Conceived and designed the experiments; Performed the experiments; Analyzed and interpreted the data; Wrote the paper.

Competing interest statement

The authors declare no conflict of interest.

Additional information

No additional information is available for this paper.

References

Adrian, R.J., 1991. Particle-imaging techniques for experimental fluid mechanics. Annu. Rev. Fluid Mech. 23 (1), 261–304.

Adrian, L., Adrian, R.J., Westrweel, J., 2011. Particle Image Velocimetry. Cambridge University Press.

Chanel, P.G., 2009. An Evaluation of Computational Fluid Dynamics for Spillway Modeling. M.Sc. Thesis. University of Manitoba, Winnipeg, Manitoba, Canada. http://hdl.handle.net/1993/3112.

Engineers, U.A. C.o., 1952. Corps of Engineers hydraulic design criteria. In: Waterways Experiment Station Vicksburg, Miss.

Fujita, I., et al., 1998. Large-scale particle image velocimetery for flow analysis in hydraulic engineering applications. J. Hydraul. Res. 36 (3), 397–414.

Ho, D.K., et al., 2006. Application of Numerical Modelling to Spillways in Australia. Taylor and Francis group, London, UK, pp. 951–959.

Kanyabujinja, P.N., 2015. CFD Modelling of Ogee Spillway Hydraulics and Comparison with Experimental Mosel Tests. M.Sc. thesis. Stellenbosch university, Stellenbosch, South Africa. http://hdl.handle.net/10019.1/96787.

Khatsuria, R.M., 2004. Hydraulics of Spillways and Energy Dissipators. CRC Press.

Kim, D.G., Park, J.H., 2005. Analysis of flow structure over ogee-spillway in consideration of scale and roughness effects by using CFD model. KSCE J. Civil Eng. 9 (2), 161–169.

Kuok, K.k., Chiu, P.C., 2017. Application of particle image velocimetry (PIV) for measuring water velocity in laboratory sedimentation tank". IRA Int. J. Technol. Eng. 9 (3), 16–26.

Maynord, S.T., 1985. General spillway investigation: hydraulic model investigation. In: Technical Report HL-85-1, US Army Engineering Waterways Experiment Station, Vicksburg, Mississippi. https://apps.dtic.mil/dtic/tr/fulltext/u2/a156686.pdf.

Peltier, Y., et al., 2015. Pressure and velocity on an ogee spillway crest operating at high head ratio: experimental measurements and validation. In: 2nd International Workshop on Hydraulic Structure. Coimbra, Portugal, pp. 128–136.

Peltier, Y., Dewals, B., Archambeau, P., Pirotton, M., Erpicum, S., 2018. Pressure and velocity on an ogee spillway crest operating at high head ratio: experimental measurements and validation. J. Hydro-Environ. Res. 19, 128–136.

Savage, B.M., Johnson, M.C., 2001. Flow over ogee spillway:experimental and numerical model case study". J. Hydraul. Eng. 127 (8), 640–649.

Sveen, J.K., Cowen, E.A., 2004. Quantitative imaging techniques and their application to wavy flows, in PIV and water waves". In: Advances in Coastal and Ocean/Engineering PIV and Water Waves. Would Scientific, pp. 1–49.

U.S. Bureau of Reclamation, 1987. Design of Small Dams. Water Resources Technical Publication, U.S. Department of the Interior, Bureau of Reclamation.

Willey, J., Ewing, T., Wark, B., Lesleighter, E., 2012. Complementary use of experimental and numerical modelling techniques in spillway design refinement. In: Commission International Des Grands Barrages,Kyoto, pp. 1–22. https://books.google.com_books_about_An_Introduction_to_Computati.

Instruction Manuals:

Instruction manual of S6-MKII, Armfield Company, 2014.

Manual of the rtCam PIV System, 2009.